Application of sensitivity analysis in DC resistivity monitoring of SAGD steam chambers

Sarah G. R. Devriese and Douglas W. Oldenburg*
Geophysical Inversion Facility, University of British Columbia

SUMMARY

Steam Assisted Gravity Drainage (SAGD) is a proven technology to extract heavy oil from the Athabasca oil sands in Alberta, Canada. Research and pilot programs have shown the growth in steam chambers can be detected and monitored using electrical methods, indicating a decrease in electrical resistivity due to steaming process. We analyze surveys currently in practice using the sensitivity of the data to model perturbations. We show that certain surveys have greater sensitivity to important regions of the reservoir, and that inversions of data collected using these surveys provide better recovery of the chambers. The sensitivity analysis provides a computationally fast and inexpensive approximation of what a full inversion can recover, making it ideal in survey design studies. Our aim is to use analysis of the sensitivity matrix to design improved surveys as well as extend the surveys to multi-frequency electromagnetic methods.

INTRODUCTION

Steam Assisted Gravity Drainage (SAGD) is an oil-extraction method used in the Athabasca oil sands in Alberta, Canada. The heavy oil, or bitumen, is too viscous to be extracted using conventional methods and is generally too deep for mining. Steam is injected into the reservoir through a horizontal well at the bottom of the reservoir. A steam chamber grows radially outwards and heats the surrounding oil, which becomes fluid and flows through the reservoir. The oil and condensed steam are collected by a second horizontal well that lies approximately 5 m below the injector. As the oil is heated and drained, the chamber continues to grow and expand into the reservoir (Butler, 1994).

Reservoir heterogeneity, such as clay and mudstone laminations, can impede steam propagation, which affects the amount of oil produced. Monitoring the chamber growth over time allows for detecting areas of no-growth, finding missed pay, and identifying thief zones. Such information aids in optimizing production and decreasing water usage. Geophysical methods are ideally suited to detect reservoir changes, with two major factors influencing the results: (1) the physical property contrasts, and (2) survey design. In the case of SAGD, as steam heats the oil, the electrical resistivity of the reservoir decreases (Mansure et al., 1993), allowing for electric and electromagnetic methods to be used to monitor the steam chamber growth (Devriese and Oldenburg, 2014). A well-designed survey is able to provide detailed information about the region of interest such that the steam chambers can be recovered using inversion. However, survey design is not trivial. Often, numerical modeling and inversion aids in determining the efficacy of survey design but three-dimensional inversions are computationally costly and take time.

In this paper, we use sensitivity analysis as a proxy for determining model resolution from a given survey design. We focus on currently in-practice crosswell DC resistivity surveys used to monitor SAGD steam chambers and identify strengths and weaknesses in each design. To validate our results, DC resistivity data are inverted in three dimensions, indicating that the sensitivity analysis provides a fast and computationally inexpensive method to judge a particular survey design without resorting to full inversions.

We focus on a field site at the Leismer Demonstration Area, which is located in the Athabasca oil sands. The area is approximately 100 km south of Fort McMurray and 120 km north of Lac La Biche. In one of the SAGD well pads, a permanent cross-well survey was installed using two vertical boreholes to monitor SAGD steam chamber growth using cross-well seismic, vertical seismic profiling, and cross-well DC resistivity. The two vertical boreholes straddle two horizontal injector and producer pairs, as shown in Figure 1. DC resistivity was collected twice a day using multiple survey orientations for four years (Tøndel et al., 2014). The results indicated a 85% decrease in resistivity due to the growth of two steam chambers over a two-year period.

GEOLOGY AND SURVEYS

We first generate a synthetic time-lapse resistivity model using the geology and acquisition parameters at the Leismer Demonstration Area. A background layered earth model is created from the baseline model from Tøndel et al. (2014) and has six distinct layers. A Quaternary-aged glacial layer extends from the surface at 650 m to approximately 340 m and is modeled using a resistivity of 20 Ωm. Below the Quaternary lies the shale-rich Clearwater Formation and acts as a cap rock for the SAGD process. This layer is modeled as approximately 80 m in thickness with a resistivity of 5 Ωm. The McMurray Formation, which is the main oil reservoir, lies below the cap rock and is comprised of multiple sections. The top and bottom sections, both modeled as 20 Ωm, are approximately 30 m thick. The middle section contains the growing steam chambers and has a thickness of 30 m. The resistivity of this section is substantially higher and is modeled as 200 Ωm. Below the McMurray, a Devonian limestone unit is modeled as 50 Ωm and starts at an elevation of 170 m. Figure 1 shows the resistivity model with the well and electrode configurations.

Four steam chambers are added to the middle McMurray Formation at the locations of the horizontal well pairs and have a resistivity of 20 Ωm. Each chamber is 20 m in the easting direction and 15 m in height, starting at an elevation of 205 m. They are modeled at a length of 280 m in the northing direction, where the center is aligned with the vertical wells at a northing of 0 m. This provides two time steps in the SAGD process: before and after steaming.

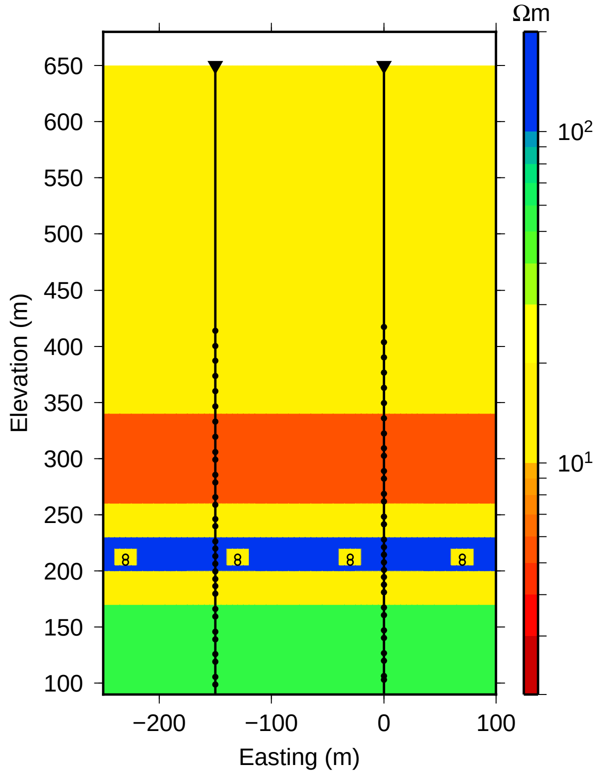

Figure 1: The geology at Leismer is modeled as a 1D layered earth with 4 SAGD chambers added. The figure shows a slice through the 3D model at a northing of 0 m. Two observation wells are located at an easting of 0 m and -150 m and contain electrodes, indicated as black dots. The horizontal well pairs, indicated using black circles, are at easting values of -230 m, -130 m, -30 m, and 70 m.

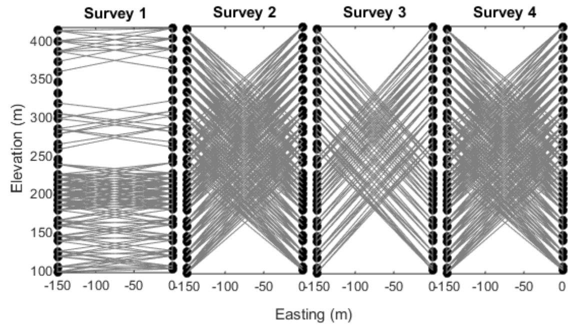

Figure 2: Four DC resistivity surveys collected at the Leismer Demonstration Area to monitor steam chamber growth. Black dots indicate electrode locations. Grey lines connect transmitter electrodes. Surveys 1, 3, and 4 also have along-well transmitters (not shown).

We use the same well configuration as Tøndel et al. (2014), where two vertical observation wells sit between the horizontal wells, as shown in Figure 1. The two vertical wells are 150 m apart. The horizontal separation between the each pair of horizontal wells is 100 m while each horizontal well pair lies at an elevation of approximately 210 m.

The observation wells reach the surface at an elevation of 650 m but the instrumentation within the wells is limited between 400 and 100 m. The electrodes are spaced every 13.5 m down each well, except in the middle McMurray Formation where they are placed every 7 m. The four surveys, shown in Figure 2, consist of (1) 169 transmitters and 5,352 data, (2) 174 transmitters and 16,928 data, (3) 125 transmitters and 8,640 data, and (4) 274 transmitters and 17,088 data. Transmitters are placed both across the two vertical wells and along the same vertical well in all surveys except Survey 2, which only has crosswell transmitters. Survey 4 is identical to Survey 2, except for the addition of 100 along-well transmitters. In addition, Survey 4, which has the most transmitters, has 54 and 82 transmitters in common with Surveys 1 and 3, respectively. Receiver electrode pairs use the same configuration as the transmitters.

ESTIMATION OF THE SENSITIVITY

The forward modeling of DC resistivity uses a steady-state version of Maxwell's equations, which are nonlinear. The general forward problem is given by:

$$\mathbf{d} = \mathscr{F}[\mathbf{m}], \quad (1)$$

where $\mathbf{d}$ is the data, $\mathbf{m}$ is a conductivity model, and $\mathscr{F}$ is the forward mapping operator. An inversion of these data would require $\mathscr{F}^{-1}$ but instead, the inverse solution is formed as an optimization problem by minimizing an objective function such that Equation 1 holds (Oldenburg and Li, 2005; Nocedal and Wright, 2006). The optimal solution is found when the derivative is at zero, giving rise to the sensitivity matrix J, defined as:

$$J = \frac{\partial \mathscr{F}[\mathbf{m}]}{\partial \mathbf{m}}. \quad (2)$$

J is a $n \times m$ matrix, where n is the number of data and m is the number of model parameters in $\mathbf{m}$. The sensitivity matrix describes how the data changes given a model perturbation. Accordingly, it directly relates the survey design to the model. For small problems, J can be directly formed and the average sensitivity for the jth cell, s_j, is calculated as follows:

$$s_j = \frac{1}{nV_j} \sum_{i=1}^{n} |J_{ij}|, \quad (3)$$

where V_J is the volume of the cell. For the inversion of DC data, J is not necessarily explicitly formed to avoid storage of the large matrix. However, we can easily form matrix-vector products using the sparse differential operators that make up Jv and $J^T w$, where v and w are vectors.

Fortunately, a measure of the average sensitivity can be determined by calculating the diagonal of $J^T J$, which is an $m \times m$ matrix. The magnitude of the entries in $J^T J$ decay away from the diagonal, thus the diagonal itself contains the majority of the sensitivity. The diagonal is viewed in the same manner as the resistivity model, providing spatial information that is easily interpretable.

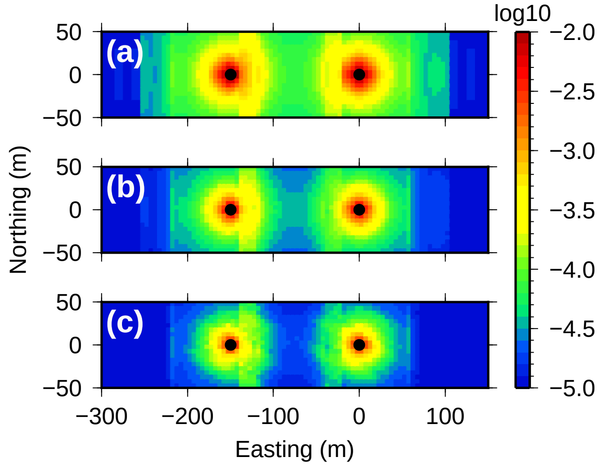

Figure 3: Plan-view section of the sensitivity at an elevation of 215 m calculated using the probing method with (a) 1, (b) 5, and (c) 15 iterations.

To calculate the diagonal of $J^T J$, Hutchinson's trace estimator uses vectors of -1 and 1 (Hutchinson, 1990) but generally requires a large number of iterations to reach an adequate result. Computation time is decreased by using the probing method: a diagonal estimator that uses pseudo-random vectors (Bekas et al., 2007). The estimator is defined as:

$$D \approx \left[\sum_{k=1}^{p} v_k \odot J^T (J v_k)\right] \oslash \left[\sum_{k=1}^{s} v_k \odot v_k\right], \quad (4)$$

where p is a user-defined number of iterations, and $\odot$ and $\oslash$ indicate component-wise vector multiplication and division, respectively. This diagonal estimator uses two matrix-vector products: $J v_k$ (which returns a vector) and $J^T (J v_k)$, and thus appeals to our problem where the sensitivity is never fully formed. The pseudo-random vectors consist of 0 and 1 and is best explained using an example. If the number of iterations p is set to 3, the pseudo-random vectors become:

$$v_1 = [1001001...]^T,$$
$$v_2 = [0100100...]^T,$$
$$v_3 = [0010010...]^T.$$

Because these pseudo-random vectors act on the structure of the matrix $J^T J$, where the diagonal has the largest magnitude, only a small number of iterations are required to reach an adequate result. In addition, if p were set to the number of model values m, then the matrix containing the v vectors becomes the identity matrix and the diagonal of $J^T J$ is recovered exactly.

SENSITIVITY ANALYSIS

The sensitivity is estimated using the probing method with the model containing the steam chambers for the four crosswell DC resistivity surveys. We tested various number of iterations to determine an acceptable number. Figure 3 shows the results for Survey 1 using 1, 5, and 15 iterations. Overall, the results are very similar with only minor details changing. Thus, even with a low number of iterations, and hence low computational cost, the probing method obtains an adequate approximation of the sensitivity matrix.

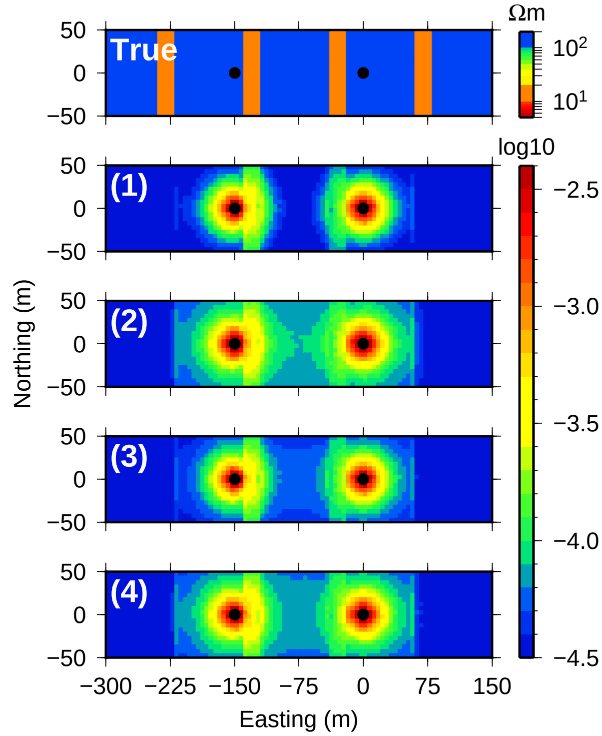

Figure 4: Plan-view sections of the sensitivity at an elevation of 215 m calculated using the probing method with 5 iterations for each of the four surveys. In each case, there is higher sensitivity to the left chamber than the right. Even though there are chambers on the other sides of the two vertical wells, none of the surveys are sensitive to those regions. The top panel shows a plan-view section through the true model, shown in Figure 1.

We approximate the sensitivity ($p = 5$) for each of the 4 surveys. Figure 4 shows that the surveys are more sensitive to the left chamber compared to the right chamber. Thus, we expect that the inversion will recover the leftmost chamber and struggle with recovering any difference in the right chamber. Additionally, Surveys 2 and 4 have a higher sensitivity to the region between the two chambers, indicating that they can distinguish better between the chambers and the unsteamed reservoir. For all four surveys, there is limited or no sensitivity to the regions outside of the two vertical wells, suggesting that these surveys do not detect the two outer steam chambers. This means that we can constrain the inversion to only allow resistivity changes between the vertical wells within the reservoir.

As the steam chambers grow, the sensitivity analysis is repeated to determine a survey's ability to detect changes in steam chamber size. Such analysis indicates how often full 3D inversions of the data are actually necessary and when a survey provides new information about steam chamber growth. If there is insignificant sensitivity to changes in the model over time, data sets can be combined and averaged to improve signal-to-noise ratios and provide better estimates of data uncertainties.

VALIDATION WITH 3D INVERSION

To validate the interpretations made from the sensitivity analysis, we forward model and invert DC resistivity data using the synthetic model in 3D for each survey (Haber et al., 2012). To simulate real data, 0.5% Gaussian noise is added. Such a low value is used assuming the data is collected repeatedly to improve signal-to-noise ratios. Uncertainties for the DC resistivity data are assigned as 0.5% percent of the data plus a noise floor of 30 mV. The layered background model was used for the initial and reference model. Additionally, only the resistivity of cells within the reservoir and between the boreholes were allowed to change. The inversion for each survey reaches target misfit and reproduces the data. We subtract the recovered models from the background model and show the results in Figure 5.

Each of the four surveys allow for both inner steam chambers to be recovered. However, the leftmost chamber has a better shape and is closer to the true resistivity value while the right chamber has a less-defined shape and is more resistive. This agrees with the observations from the sensitivity analysis: we expected to be able to recover the left chamber better than the right chamber. Without the sensitivity analysis, the recovered models can be misinterpreted as having less steam, and thus a lower decrease in resistivity. This exemplifies the importance of adequate survey design and using the sensitivity analysis to understand what the data are sensitive to.

Additionally, we see that in between the two chambers, each survey shows different amounts of structures. It is equally important to have sensitivity to the middle portion to accurately recover the reservoir. The sensitivity for Survey 4 shows higher values in between the two chambers, which results in better separation between the two chambers compared to the other surveys. Recall that Surveys 2 and 4 were identical, except for the addition of along-well transmitters. The recovered models using Surveys 3 and 4 distinguish the two chambers much better than using Surveys 1 and 2, indicating the importance of using both along-well and large-offset crosswell transmitters. This information allows us to select specific surveys that improve the ability to detect and monitor steam chamber growth.

CONCLUSION

We used sensitivity analysis on four currently-used survey designs to understand how well each survey detects two SAGD steam chambers. The sensitivity analysis is computationally inexpensive and fast compared to full inversion and provides adequate information to judge the strengths and weaknesses of a particular survey design. The sensitivity interpretations were validated by inverting synthetic data for each survey. All four surveys recovered the chambers through 3D inversion, with the left-most chamber being better defined, as expected from the sensitivity analysis. The analysis also indicated that surveys are not highly sensitive to the right-most chamber, which the inversions struggled to recover. The analysis prevented misinterpretation of the inversion model. The small difference in resistivity did not indicate a low presence of steam but rather was due to lack of sensitivity to the right steam chamber. Sensitivity analysis thus quickly provides estimates of the efficacy of a particular survey design during feasibility modeling, promoting the creation of superior surveys. The approximate sensitivity methodology also easily translates to other SAGD sites as the locations of the horizontal injector and producer are well known. Synthetic chambers should be added in those locations to calculate the approximate sensitivity, as done here. Additionally, the method can be applied to other geophysical surveys, such as electromagnetic methods, to better understand the appropriateness of a particular survey design and improve recovery of both steam chambers.

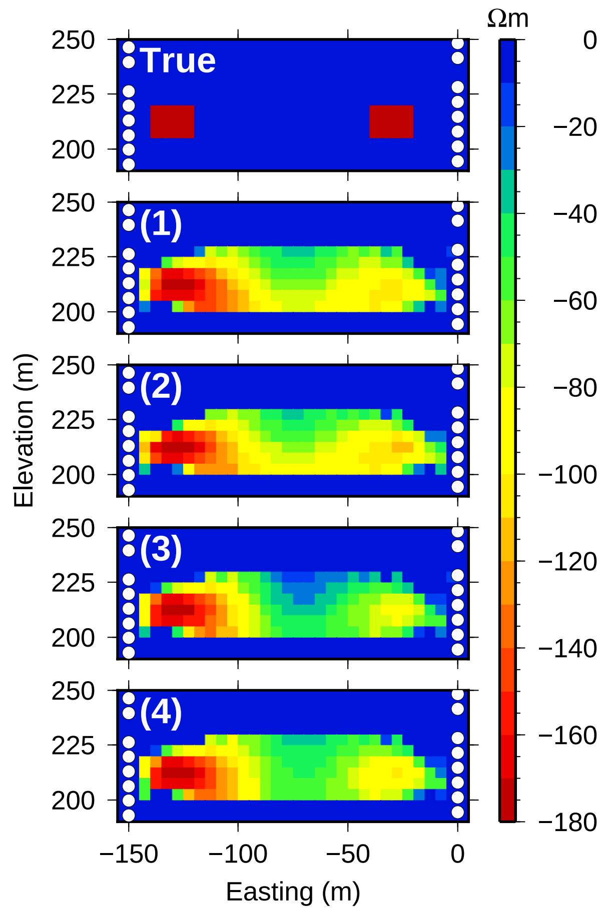

Figure 5: Each panel shows the recovered models at a northing of 0 m for the four different surveys. Only the reservoir portion is shown as only these cells were allowed to change resistivity in the inversion. Color scale indicates the change in Ωm from the initial model.

ACKNOWLEDGMENTS

We would like to thank Statoil for the data for this research project.

EDITED REFERENCES

Note: This reference list is a copyedited version of the reference list submitted by the author. Reference lists for the 2016 SEG Technical Program Expanded Abstracts have been copyedited so that references provided with the online metadata for each paper will achieve a high degree of linking to cited sources that appear on the Web.

REFERENCES

Bekas, C., E. Kokiopoulou, and Y. Saad, 2007, An estimator for the diagonal of a matrix: Applied Numerical Mathematics, **57**, 1214–1229, http://dx.doi.org/10.1016/j.apnum.2007.01.003.

Butler, R. M., 1994, Steam-assisted Gravity Drainage: Concept, Development, Performance and Future: Journal of Canadian Petroleum Technology, **33**, 44–50, http://dx.doi.org/10.2118/94-02-05.

Devriese, S. G. R., and D. W. Oldenburg, 2015, Time-lapse three-dimensional electromagnetic inversion of growth-impeded SAGD steam chambers: 85th Annual International Meeting, SEG, Expanded Abstracts, 2842–2847, http://dx.doi.org/10.1190/segam2015-5909921.1.

Haber, E., J. Granek, D. Marchant, E. Holtham, D. Oldenburg, and R. Shekhtman, 2012, 3D inversion of DC/IP data using adaptive OcTree meshes: 82nd Annual International Meeting, SEG, Expanded Abstracts, 1–5, http://dx.doi.org/10.1190/segam2012-1438.1.

Hutchinson, M. F., 1990, A stochastic estimator of the trace of the influence matrix for Laplacian smoothing splines: Communications in Statistics - Simulation and Computation, **18**, 1059–1076, http://dx.doi.org/10.1080/03610919008812866.

Mansure, A. J., R. F. Meldau, and H. V. Weyland, 1993, Field Examples of Electrical Resistivity Changes During Steamflooding: SPE Formation Evaluation, **8**, 57–64. http://dx.doi.org/10.2118/20539-PA.

Nocedal, J., and S. Wright, 2006, Numerical Optimization: Springer.

Oldenburg, D. W., and Y. Li, 2005, Near-Surface Geophysics; SEG, Ch. 5, 59–150.

Tøndel, R., H. Schutt, S. Dummong, A. Ducrocq, R. Godfrey, D. LaBrecque, L. Nutt, A. Campbell, and R. Rufino, 2014, Reservoir monitoring of steam-assisted gravity drainage using borehole measurements: Geophysical Prospecting, **62**, 760–778, http://dx.doi.org/10.1111/1365-2478.12131.